Effect of resistivity on the MHD pedestal stability in JET

H. Nyström[1], L. Frassinetti[1], S. Saarelma[2], G.T.A. Huijsmans[3], C. Perez von Thun[4], C.F. Maggi[2], J.C. Hillesheim[2] and JET contributors*
[1] Division of Fusion Plasma Physics, KTH, Stockholm, Sweden
[2] CCFE, Culham Science Centre, Abingdon, OX14 3DB, United Kingdom of Great Britain and Northern Ireland
[3]CEA, IRFM, 13108 Saint-Paul-Lez-Durance, France
[4]Institute of Plasma Physics and Laser Microfusion (IPPLM), Hery 23, 01-497 Warsaw, Poland
*See the author list of J. Mailloux et al. Nucl. Fusion 2022 https://doi.org/10.1088/1741-4326/ac47b4

The pedestal in type I ELMy plasmas is commonly accepted to be limited by ideal peeling-ballooning modes. However, recent JET results obtained in type I ELMy H-modes have shown that the ELM can be triggered also before the ideal peeling-ballooning boundary is reached [1, 2, 3]. In terms of engineering parameters, this typically occurs at high power and high gas rate [2] or, in terms of physics parameters, at high relative shift between the density and temperature pedestals [4]. More recently, the disagreement between experimental results and ideal MHD predictions has been correlated with the resistivity in the middle-bottom of the pedestal [5]. This correlation indicates that resistive MHD might be required to describe the pedestal in plasmas with high relative shift.

In this work, we present the initial results of including resistivity on the MHD stability analysis of an extended JET dataset. In the stability analysis the CASTOR [6] code has been used. The CASTOR code is a linear MHD eigenvalue solver that includes resistivity but does not include diamagnetic effects. The effect of the diamagnetic stabilization is therefore implemented as a critical limit in the growth rate, taken as $\gamma = 0.25\omega^*_{max}$ where ω^*_{max} is the maximum diamagnetic frequency in the pedestal.

The work is focused on two parts. Firstly, the detailed analysis of two different shots with differing gas and power, to understand the effect resistivity has on the peeling-ballooning stability. Secondly, a larger dataset is considered to see if the results obtained in the detailed analysis can be generalized to other shots.

The datasets that have been considered in this work are a JET-ILW low triangularity gas and power scan at 1.4MA/1.7T and a gas scan at constant β_N at 2MA/2.3T with shots from both JET-ILW and JET-C. Two shots from the gas and power scan at 1.4MA/1.7T have been studied in greater detail. The first of these is shot 84793, which is a shot at low power and low gas rate ($P_{NBI} \sim 4.5$MW, $\Gamma_{D2} \sim 2.7\times10^{21}$es^{-1}) that is ideally PB-limited (hereafter called LPLG). The second is shot 87342, which is a shot at high power and high gas rate ($P_{NBI} \sim 15$MW, $\Gamma_{D2} \sim 18\times10^{21}$es^{-1}) that is not ideally PB-limited (hereafter called HPHG).

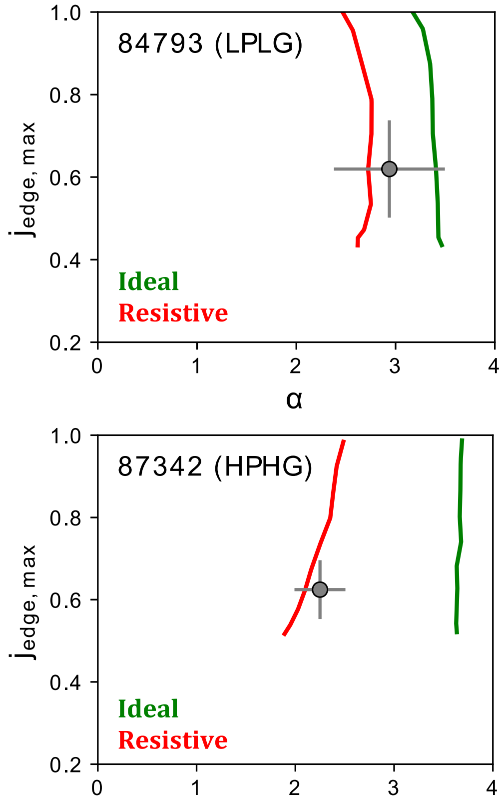

Figure 1. Stability boundary in j-α space including (red) and excluding resistivity (green). Experimental point is shown with errorbars in grey. (a) #84793 (LPLG) (b) #87342 (HPHG)

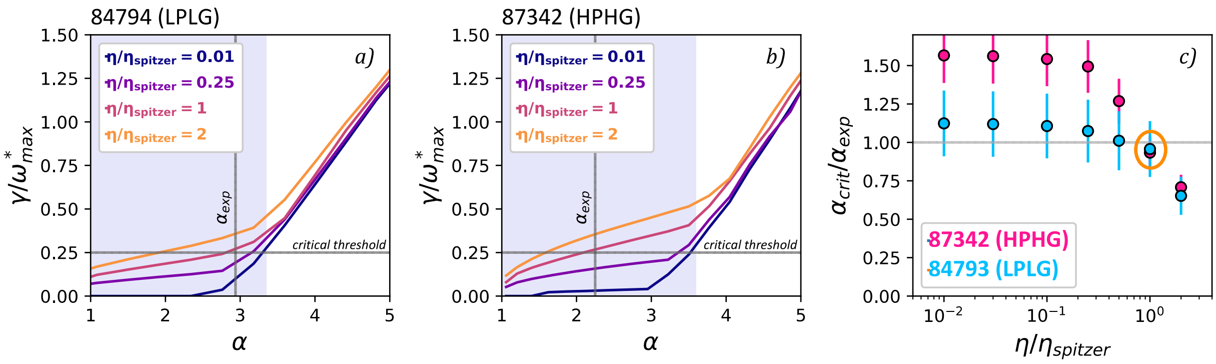

Figure 2. Effect of uniformly rescaling the resistivity profile on the growth rate of the most unstable mode for LPLG (a) and HPHG (b) and the resulting impact on $\alpha_{crit}/\alpha_{exp}$ (c).

The stability boundary in j-α space for the LPLG and HPHG cases can be seen in figure 1. In the figure it can be seen that the inclusion of resistivity has a moderate effect on the stability boundary of the LPLG case and that the stability boundary remains within the uncertainty of the experimental point. For the HPHG case the effect on the stability boundary from including resistivity is larger. In particular, it moves the stability boundary from being far from the experimental point to within experimental uncertainty. Resistive MHD thereby seems to be able to explain the location of the experimental point for these two cases.

To understand the effect of including resistivity a scan has been performed where the resistivity has been incrementally increased by uniformly rescaling the experimental resistivity profile for the LPLG and HPHG cases. This has been done at constant j_{edge} while artificially modifying the pressure gradient in order to find the critical α. The results are shown in figure 2. For both the LPLG and HPHG cases we can see that increasing the resistivity has a relatively week effect on the ideally unstable region (the white area). In the ideally stable region (the light blue area), the growth rates are instead highly sensitive to the increasing resistivity. When the growth rates in this region start reaching the critical threshold we then start getting a modification of the critical α. The resistivity scaling factor where this starts happening is however different for the LPLG and HPHG cases as can be seen in figure 2c) where α_{crit} starts being affected at a scaling factor of ~0.2 for HPHG and at the experimental resistivity for the LPLG case.

It is of course paramount to quantify how sensitive the results shown here are to uncertainties in key parameters. Therefore, the results of two sensitivity tests are shown in figure 3. The first is the effect on $\alpha_{crit}/\alpha_{exp}$ from a 40% change in the electron separatrix temperature which is shown in a). The electron separatrix temperature has been modified by shifting the temperature and density profiles radially to reach the specified separatrix temperature. As can be seen the effect on the HPHG case is negligible while the effect on LPLG is at most ~20%.

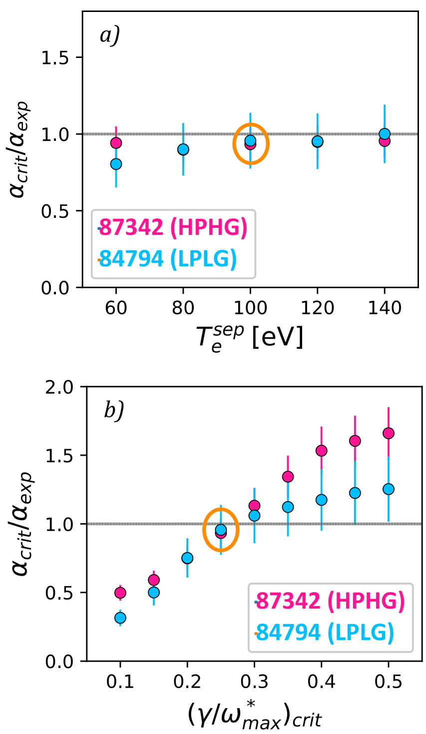

Figure 3. Effect on $\alpha_{crit}/\alpha_{exp}$ *of LPLG and HPHG from changing the electron separatrix temperature (a) and the critical threshold (b).*

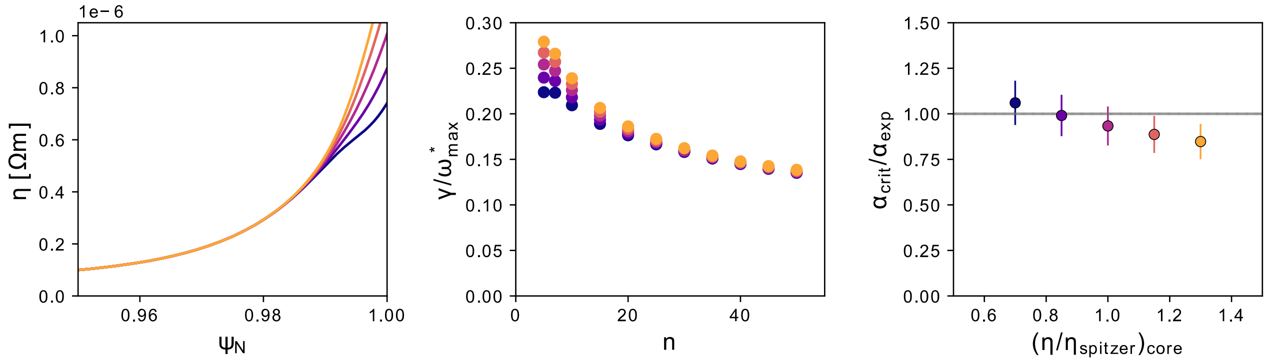

Figure 4. Effect of changing the resistivity profile of HPHG according to (a) on the growth rate of various toroidal modes (b) and the resulting $\alpha_{crit}/\alpha_{exp}$ (c).

The second sensitivity test is related to the critical threshold used to approximate the diamagnetic stabilization. As the growth rates in the ideally stable region are less strongly dependent on α, the sensitivity to the critical threshold will be larger compared to the ideal MHD predictions. The results of a variation of $(\gamma/\omega^*_{max})_{crit}$ from 0.1 to 0.5 can be seen in figure 3b) where there is a strong effect on $\alpha_{crit}/\alpha_{exp}$. As the critical threshold is increased, $\alpha_{crit}/\alpha_{exp}$ approaches the ideal prediction for the same critical threshold. As the critical threshold is reduced however, $\alpha_{crit}/\alpha_{exp}$ will tend towards zero as the entire first ballooning stability region can be expected to have finite growth rates when resistivity is included. A proper treatment of the diamagnetic effects will be an important continuation to validate the results of the present work.

The question now arises of where the resistivity is most important. To investigate this, the resistivity has been changed locally to assess the impact on the various toroidal modes and on $\alpha_{crit}/\alpha_{exp}$. The results of varying the resistivity profile at the very edge of the HPHG case can be observed in figure 4. In 4a) the modified resistivity profiles are shown while 4b) highlights the growth rates of the toroidal modes for the different resistivity profiles and 4c) the resulting $\alpha_{crit}/\alpha_{exp}$. The low *n* modes, that are the most unstable when resistivity is included, are highly edge localized and destabilized by increasing the resitivity at the very edge. The larger *n* modes have much larger radial extent however and are therefore not as destabilized by increasing the resistivity in this region. A similar test has been performed by changing the resistivity near the pedestal top (not shown here). In this case, no significant effect on $\alpha_{crit}/\alpha_{exp}$ is observed. These results are consistent with the fact that the correlation between $\alpha_{crit}/\alpha_{exp}$ and resistivity was only observed for the resistivity at the middle-bottom of the pedestal [5] (last 2% in Ψ_N).

Including resistivity seems to be able to explain the location of the experimental point for both the LPLG and HPHG cases. To see if this holds when larger datasets are considered, constant j_{edge} scans have been performed for the datasets described in the introduction. The results can be seen in figure 5 where $\alpha_{crit}/\alpha_{exp}$ has been plotted versus the relative shift between the electron temperature and

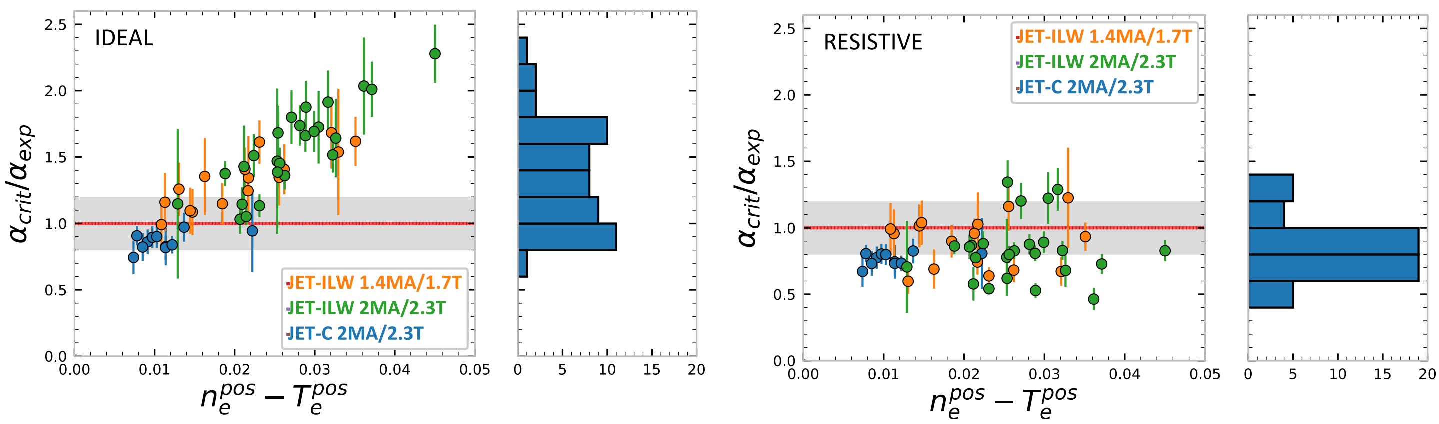

Figure 5. $\alpha_{crit}/\alpha_{exp}$ versus the relative shift between the electron temperature and density pedestal using ideal MHD (a) and including resistivity (b) histograms clarify the distribution of the data points.

density pedestals. Figure 5a) shows the results using ideal MHD and 5b) shows the results including resistivity. In a) there is a very clear systematic trend between $\alpha_{crit}/\alpha_{exp}$ and the relative shift which is consistent with previous works where much larger datasets have been considered [3]. When resistivity is included, the agreement between model and experiment is significantly improved. In particular the trend between $\alpha_{crit}/\alpha_{exp}$ and the relative shift is removed. There is also a slight reduction in $\alpha_{crit}/\alpha_{exp}$ for the cases that are already ideally PB-limited but it is the cases with large relative shifts that are the most affected by the inclusion of resistivity. It is also interesting to note that the most unstable mode is in general shifted towards lower mode numbers when resistivity is included in the analysis. This can be clearly seen in figure 6a) where the most unstable mode of the entire dataset is plotted versus the relative shift using ideal MHD (empty triangles) and including resistivity (filled circles). The inclusion of resistivity shifts the most unstable mode towards lower *n* and in particular, closer to the range of experimentally observed ELM precursors marked by the grey band. An example of these ELM precursors can be seen in figure 6b).

The present results have similarities with a recent work using JOREK to study the role of resistivity in small ELM regimes at AUG [7]. In the work, it was shown that the inclusion of resistivity could explain the ELM triggering mechanism as caused by resistive peeling ballooning modes.

The results of this work shows that the inclusion of resistivity could be necessary to describe the ELM triggering mechanism in JET. In particular, the systematic trend between $\alpha_{crit}/\alpha_{exp}$ and the relative shift that has been consistently seen in JET-ILW is removed and the agreement with experiment is significantly improved.

This work has been carried out within the framework of the EUROfusion Consortium, funded by the European Union via the Euratom Research and Training Programme (Grant Agreement No 101052200 — EUROfusion). Views and opinions expressed are however those of the author(s) only and do not necessarily reflect those of the European Union or the European Commission. Neither the European Union nor the European Commission can be held responsible for them.

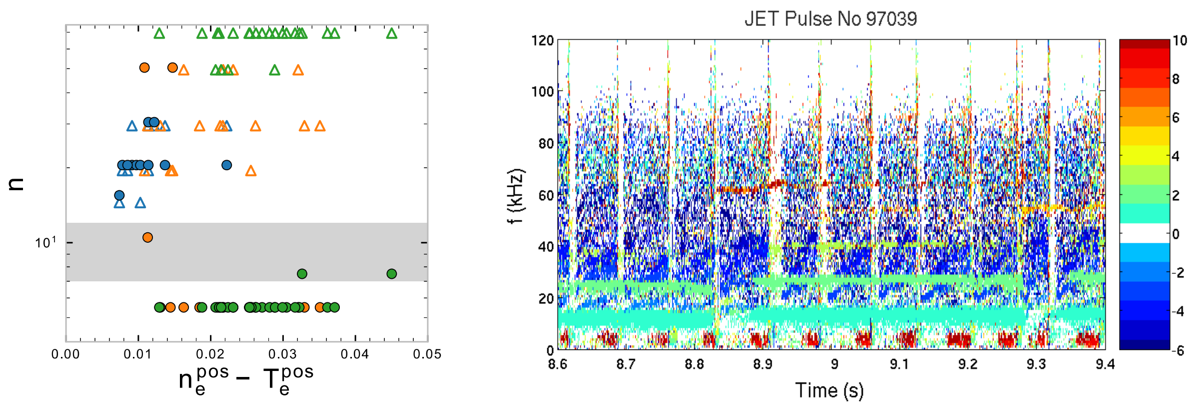

Figure 6. The most unstable mode (a) using ideal MHD (empty triangles) and including resistivity (filled circles). The grey region marks the range of observed experimental ELM precursors. An example of this analysis can be seen in (b) where the ELM precursors are the red/orange signatures at ~5kHz before the ELMs

References

[1] M. Beurskens *et al* 2014 Nucl. Fusion **54** 043001
[2] C.F. Maggi *et al* 2015 Nucl. Fusion **55** 113031
[3] L. Frassinetti *et al* 2021 *Nucl. Fusion* **61** 016001
[4] E. Stefanikova *et al* 2018 *Nucl. Fusion* **58** 056010
[5] L. Frassinetti *et al* 2021 *Nucl. Fusion* **61** 126054
[6] W. Kerner *et al* 1998 *J. Comput.. Phys.* **142**
[7] A. Cathey *et al* 2022 *Plasma Phys. Control. Fusion* **64** 054011